Est. 1984

ORIENTAL JOURNAL OF CHEMISTRY
An International Open Free Access, Peer Reviewed Research Journal

www.orientjchem.org

ISSN: 0970-020 X
CODEN: OJCHEG
2018, Vol. 34, No.(4):
Pg. 1878-1883

Improvement in Crystallizability and Melt Flow Property of Linear Poly(L-lactide) Bioplastic by Blending with Star-shaped Poly(L-lactide)

YODTHONG BAIMARK* and YAOWALAK SRISUWAN

Biodegradable Polymers Research Unit, Department of Chemistry and Center of Excellence for Innovation in Chemistry, Faculty of Science, Mahasarakham University, Mahasarakham 44150, Thailand.
*Corresponding author E-mail: yodthong.b@msu.ac.th

http://dx.doi.org/10.13005/ojc/3404022

(Received: January 08, 2018; Accepted: June 03, 2018)

ABSTRACT

This research focuses on the crystallizability and melt flow property of linear poly(L-lactide) (1-PLL) by blending with star-shaped 16-arm PLL (16-PLL). The 1-PLL/16-PLL blends were chain extended during melt blending using an epoxy-based chain extender. The crystallinities of the 1-PLL/16-PLL blends increased with the 16-PLL blend ratio and chain extension reaction. The 16-PLL enhanced formation of branched PLL during chain extension was confirmed by thermogravimetry, and improved the melt flow property of the blends. Stresses at break of the compressed blend films were improved slightly by the 16-PLL blending and chain extension. In conclusion, the 16-PLL could be used as a nucleating agent and a melt strength enhancer for linear PLL.

Keywords: Biodegradable polymer, Poly (L-lactide) PLL, Star-shaped polymer, Crystallization, Melt flow index

INTRODUCTION

Poly(L-lactic acid) (PLA) or poly(L-lactide) (PLL) is a biodegradable bioplastic that has attracted increasing attention for use in commodity applications because of its bio-renewability, biodegradability, biocompatibility, good processability and good mechanical properties.[1-4] PLL has raised a lot of interest as a potential replacement for petroleum-based plastics. However, PLL exhibits a slow crystallization rate and low crystallinity.[5-6] Therefore, PLL products in conventional melt processes are mostly amorphous, which greatly limits its practical applications.[5,7] Many efforts have been made to improve PLL crystallizability. Addition of nucleating agents is the most economic and practical approach. The nucleating agents decrease the nucleation induction time and increase the number of primary nucleation sites.[5]

It is well known that linear PLL has a low melt viscosity.[8-9] The melt flow property of PLL has been improved by reacting with epoxy-based chain extenders to form as long-chain branched structures of PLL.[9] Moreover the epoxy-based chain extender can restore the molecular weight of PLL during melt process.[10,11] The star-shaped 4-arm PLLs have been used as homogeneous nucleating agents by solution blending with the commercial PLL to enhance crystallization and melt flow property of the PLL.[12] The branch points of the star-shaped PLL could act as nucleation sites. Meanwhile chain entanglements of the star-shaped PLL restricted chain mobility during melt flow state. However, the effects of star-shaped 16-arm PLL blending and chain extension reaction on the crystallizability and melt flow property of the linear PLL have not yet been reported.

Thus, the purpose of this work is to study the effect of the 16-arm PLL and epoxy-based chain extender on the thermal and melt flow property of linear PLL. We synthesized linear PLL (1-PLL) and 16-arm PLL (16-PLL). Then, the PLL blends with 1-PLL/16-PLL ratios of 100/0, 90/10, 80/20 and 60/40 (w/w) were prepared by melt blending.

EXPERIMENTAL

Materials

L-Lactide (LL) monomer was produced from L-lactic acid (90%, Purac) by a directly polycondensation followed with a thermal decomposition.[13] The LL was purified by repeated re-crystallization for four times with ethyl acetate. The purified LL was then dried in vacuo at 50°C for 48 h before use. 1-dodecanol (98%, Fluka) was used as an initiator containing one hydroxyl end-group. It was purified by distillation under reduced pressure before use. Boltorn® H20 (Perstorp Specialty Chemicals) was used as an initiator containing 16-hydroxyl end-groups. It was dried in vacuo at room temperature for 24 h before use. The molecular structures of 1-dodecanol and Boltorn® H20 are illustrated in Fig. 1. Stannous octoate ($Sn(Oct)_2$, 95% Sigma) was used without further purification. A styrene-acrylic multi-functional-epoxide oligomeric agent (Joncryl® ADR 4368, supplied by BASF, Thailand) with a molecular weight of 6,800 g/mol was used as a chain extender. All reagents used were analytical grade.

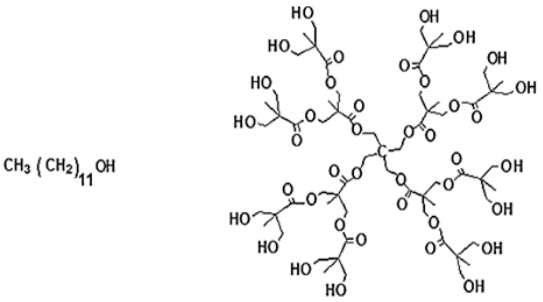

Fig. 1. Molecular structures of initiators contained one hydroxyl (1-dodecanol) and 16-hydroxyl (Boltorn® H20) end-groups

Synthesis of linear and star-shaped poly(L-lactide)

Linear poly(L-lactide) (1-PLL) and 16-arm star-shaped PLL (16-PLL) were synthesized by ring-opening polymerization of a LL monomer in bulk under a nitrogen atmosphere. The 0.01 mol% stannous octoate ($Sn(Oct)_2$, 95%, Sigma) and hydroxyl compounds was used as the initiating systems. The polymerization temperature and time were 165°C for 2.5 h, respectively. The polymerization reaction is presented in Fig. 2. The 1-dodecanol (0.14 mol%) and Boltorn® H20 (0.018 mol%) were used as the hydroxyl compounds to synthesize the 1-PLL and 16-PLL, respectively. The obtained PLLs were granulated and dried in vacuo at 110°C for 2 h to remove any un-reacted LL monomer.

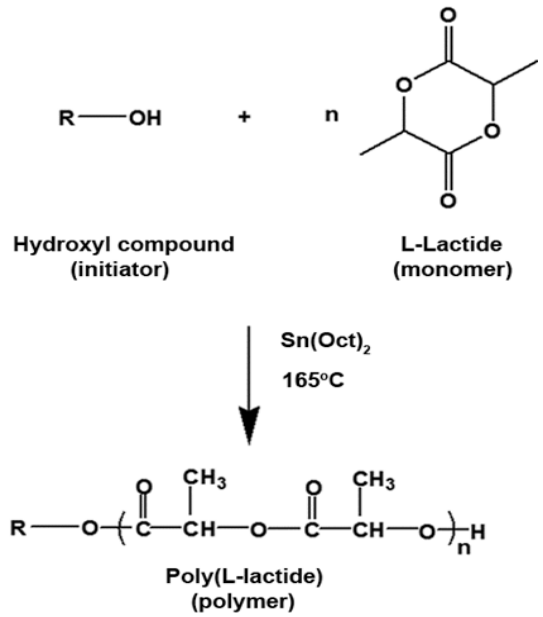

Fig. 2. Ring-opening polymerization of L-lactide monomer

The intrinsic viscosities ([η]) of the 1-PLL and 16-PLL determined in chloroform at 25°C were 2.53 and 2.54 dL/g, respectively. The L-enantiomer contents of the 1-PLL and 16-PLL obtained by the polarimetry in chloroform at 25°C were 96.5% and 96.2%, respectively. The melting temperatures (T_m) of the 1-PLL and 16-PLL were 174 and 175°C, respectively as determined by differential scanning calorimetry (DSC).

Preparation of 1-PLL/16-PLL blends

The 1-PLL, 16-PLL and Joncryl® chain extender were dried in vacuo at 50°C overnight before melt blending. The dried 1-PLL, 16-PLL and Joncryl® (1.0 phr) were in situ melt blended to prepare chain extended 1-PLL/16-PLL blends using a HAAKE Polylab OS Rheomix batch mixer system at 190°C for 5 min. with a rotor speed of 100 rpm. The blends with 1-PLL/16-PLL blend ratios of 100/0, 90/10, 80/20 and 60/40 (w/w) were investigated. The non-chain extended 1-PLL/16-PLL blends were also prepared for comparison. The resulting 1-PLL/16-PLL blends were granulated and dried in vacuo at 50°C overnight before characterization and compression molding.

Characterization of 1-PLL/16-PLL blends

The thermal transition properties of the 1-PLL/16-PLL blends were determined using a Perkin-Elmer Pyris Diamond differential scanning calorimeter (DSC) under a nitrogen atmosphere. For DSC, ~5 mg of each sample were heated from 0°C to 200°C at 10oC/min. (1st heating scan) to remove thermal history. Then, the samples were quenched to 0°C according to the DSC instrument's own default cooling mode before heating from 0 to 200°C (2nd heating scan). The DSC results were investigated from the 2nd heating scan curves. The degree of crystallinity (X_c) of the blends was calculated from the enthalpies of melting (ΔH_m) and cold crystallization (ΔH_{cc}) using equation (1).

$$Xc(\%)=[(\Delta H_m-\Delta H_{cc})/93.7J/g]\times100 \quad (1)$$

Where ΔH_m and ΔH_{cc} were resulted from the 2nd heating DSC curves. The enthalpy of melting for 100% X_c of the PLL was 93.7 J/g.[13]

The thermal stability of the 1-PLL/16-PLL blends was measured using a TA-Instrument SDT Q600 thermogravimetric analyzer (TGA) in a non-isothermal mode. For TGA analysis, ~5 mg of each sample were scanned from 50 to 800°C at a heating rate of 20°C/min. under a nitrogen atmosphere to assess the temperature of maximum decomposition rate ($T_{d, max}$).

The melt flow index (MFI) of the 1-PLL/16-PLL blends was determined using a Tinius Olsen MP1200 melt flow indexer at 190°C with a 2.16 kg load. A 100 g rod was used as a plunger. The MFI was averaged from at least five measurements.

Tensile properties, including Young's modulus, stress at break and elongation at break, of the 1-PLL/16-PLL blend films were analyzed at 25°C and 65% relative humidity with a Lloyds LRX+ Universal Mechanical Testing Machine. The 1-PLL/16-PLL blend films were prepared using an Auto CH Carver laboratory press at 190°C without compression force for 2 min. followed with a 5 ton compression force for 2 minute. The film thicknesses were around 0.2 – 0.3 mm. The films were stored at room temperature for 24 h before tensile test. The film samples with size 100 x 10 mm were determined. A gauge length and a crosshead speed of 50 mm and 50 mm/min. were chosen. The averaged tensile properties were obtained from at least five determinations for each sample.

RESULTS AND DISCUSSION

The commercial PLL readily reacted with a chain extender to form long-chain branched structures to adjust its melt flow property for each conventional melt process. In this work, the non-chain extended 1-PLL and 16-PLL were then synthesized for clear investigation the effect of the chain extension reaction on blend properties. The 1-PLL and 16-PLL synthesized by the ring-opening polymerization were melt blended at 190°C to prepare the 1-PLL/16-PLL blends with and without chain extension.

Thermal transition properties

The DSC curves were used to study thermal transition properties of the blends, as shown in Fig. 3. All the non-chain extended and chain extended 1-PLL/16-PLL blends exhibited similar glass transition temperatures (T_g), cold crystallization temperatures (T_{cc}) and melting temperatures (T_m)

in ranges 53 - 57°C, 93 - 99°C and 173 - 175°C, respectively. The DSC results are summarized in Table 1, including the ΔH_{cc}, ΔH_m and X_c.

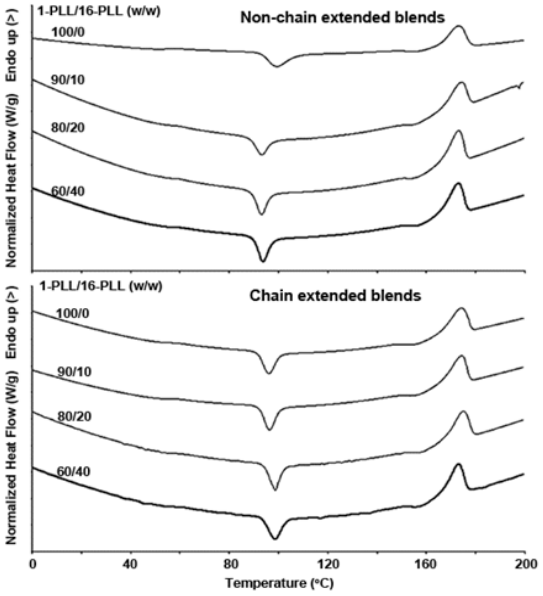

Fig. 3. Second heating scan DSC curves of (above) non-chain extended and (below) chain extended 1-PLL/16-PLL blends

Table 1: Thermal transition properties of 1-PLL/16-PLL blends from second heating scan DSC cur ves

1-PLL/16-PLL ratio (w/w)	Tg (°C)	Tcc (°C)	DHcc (J/g)	Tm (°C)	DHm (J/g)	Xc (%)
Non-chain extended blend						
100/0	53	99	28.6	173	39.1	11.2
90/10	55	93	25.9	174	40.4	15.5
80/20	56	93	27.1	173	44.9	19.0
60/40	56	94	27.2	173	48.3	22.5
Chain extended blend						
100/0	55	96	27.0	174	48.2	22.6
90/10	55	96	27.1	174	49.6	24.0
80/20	57	98	27.2	175	51.2	25.6
60/40	57	98	27.4	173	55.4	29.9

The 16-PLL blending and chain extension reaction did not significantly change the values of T_g, T_{cc}, ΔH_{cc} and Tm. However, both the ΔH_m and X_c of the non-chain extended and chain extended 1-PLL/16-PLL blends increased steadily with the 16-PLL ratio. The chain extended 1-PLL/16-PLL blends exhibited higher Xc values than the non-chain extended 1-PLL/16-PLL blends for the same blend ratio. Therefore the 16-PLL blending and chain extension improved crystallization of the blends. The results can be attributed to the star-shaped structures of 16-PLL that might have acted as nucleating sites for PLL crystallization.[5,14] The long-chain branched structures of PLL obtained from chain extension reaction also enhanced PLL crystallization.[15, 16]

Thermal stability

The thermal stability of the blends was determined from derivative thermogravimetric (DTG) curves, as shown in Fig. 4. All the non-chain extended and chain extended 1-PLL/16-PLL blends completely thermal-decomposed based on weight loss profile in the range 250 – 400°C. The peak of the DTG curves shows the Td, max. The non-chain extended 1-PLL/16-PLL blends exhibited similar DTG curves containing main T_d, max peaks and shoulder peaks in ranges 367 – 372°C and 296 – 324°C, respectively, which attributed to the thermal decomposition of shorter and longer PLL chains, respectively.[16] These were related to chain end "unzipping" mechanism of the PLL chains.[17]

Moreover, the chain extended 1-PLL/16-PLL blends illustrated similar DTG curves containing the main and shoulder T_d, max peaks in ranges 329 – 330°C and 369 – 371°C, respectively, except the 60/40 (w/w) 1-PLL/16-PLL blends that had only the lower T_d, max peak at 330°C. The intensities of the lower Td, max peaks steadily increased with the 16-PLL blend ratio for the chain extended 1-PLL/16-PLL blends. It has been reported that the T_d, max peak of the PLL with long-chain branched structures was lower than the linear PLL.[16] The chain extended 60/40 (w/w) 1-PLL/16-PLL blends exhibited only a single lower Td, max. This indicates the long-chain branched PLL was completely formed. The higher T_d, max peak of the longer linear PLL then disappeared. The DTG results indicated that the 16-PLL blending enhanced branching formation of the 1-PLL/16-PLL blends through chain extension due to its 16-hydroxyl end-groups.

Melt flow index

The melt flow property of the polymer is an important factor for considering appropriate melt process. In this study the melt flow property of the 1-PLL/16-PLL blends was observed from melt flow

index (MFI). Lower MFI is related to higher resistance of melt flow. Fig. 5 shows the MFI values of the 1-PLL/16-PLL blends that decreased steadily as the 16-PLL blend ratio increased. The MFI of chain extended 1-PLL/16-PLL blends were lower than the non-chain extension. It can be concluded that both the 16-PLL blending and chain extension reaction improved melt flow property of the blends due to the star-shaped and the long-chain branched structures, respectively.[11-12] These structures induced chain entanglement during melt flow.

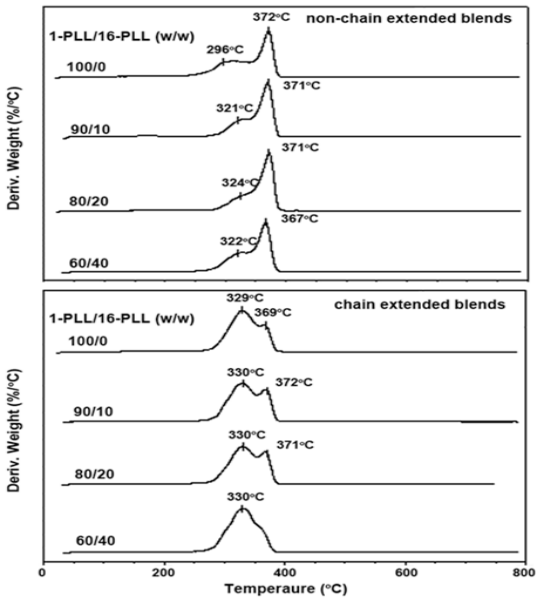

Fig. 4. DTG curves of (above) non-chain extended and (below) chain extended 1-PLL/16-PLL blends

Mechanical properties

The mechanical properties of the 1-PLL/16-PLL blend films were determined from tensile

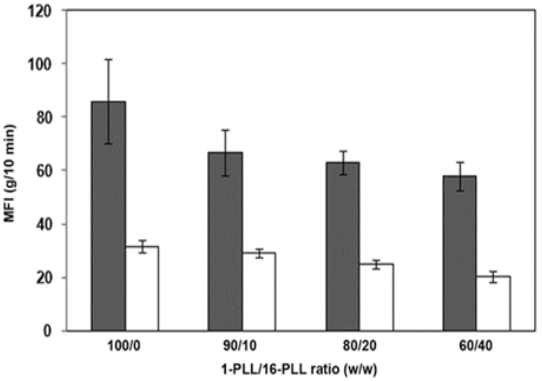

Fig. 5: MFI values of (■) non-chain extended and (□) chain extended 1-PLL/16-PLL blends

properties, as reported in Table 2. The Young's modulus of the blend films was not changed with the 16-PLL blend ratio. The Young's modulus of the non-chain extended and chain extended 1-PLL/16-PLL blend films were similar in ranges 1,065 – 1,157 and 1,323 – 1,465 MPa, respectively. The Young's modulus of the blend films were increased when the blends were chain extended with Joncry® for the same 1-PLL/16-PLL blend ratio. The long-chain branched structures suppressed elasticity of the PLL.

The stress at break of the non-chain extended and chain extended 1-PLL/16-PLL blend films increased slightly with the 16-PLL blend ratio. The chain extension reaction also improved stress at break of the blend films. They were 42.4 – 50.2 and 53.7 – 57.2 MPa for the non-chain extended and chain extended 1-PLL/16-PLL blend films, respectively. This might be due to the entanglement of star-shaped structures of 16-PLL and long-chain branched structures of chain extended 1-PLL/16-PLL blends during tensile deformation.

Table 2: Tensile properties of 1-PLL/16-PLL blends

1-PLL/16-PLL ratio (w/w)	Young's modulus (MPa)	Stress at break (MPa)	Elongation at break (%)
Non-chain extended blends			
100/0	1,100 ± 89	42.4 ± 6.9	5.9 ± 0.3
90/10	1,108 ± 80	46.7 ± 4.1	6.1 ± 1.6
80/20	1,065 ± 142	50.2 ± 1.7	6.5 ± 1.4
60/40	1,157 ± 92	49.9 ± 3.6	6.4 ± 0.8
Chain extended blends			
100/0	1,465 ± 71	53.7 ± 5.2	5.7 ± 0.5
90/10	1,365 ± 160	55.8 ± 4.7	6.2 ± 1.5
80/20	1,323 ± 161	56.3 ± 4.8	6.3 ± 1.1
60/40	1,393 ± 124	57.2 ± 3.2	6.2 ± 1.2

The elongation at break of the non-chain extended and chain extended 1-PLL/16-PLL blends with various blend ratios were similar in range 5.7 – 6.5%. The 16-PLL blending and chain extension did not change the elongation at break of blend films. The results of the mechanical properties suggest that the 16-PLL blending improved only stress at break of the blend films. However, an increase of both the Young's modulus and stress at break of the blend films were obtained by chain extension reaction.

CONCLUSION

This work reveals the beneficial effects of 16-PLL and chain extension reaction on the properties of 1-PLL. The 1-PLL/16-PLL blends were prepared by melt blending. The crystallinities of PLL blends increased with the 16-PLL blend ratio and chain extension. From TGA analysis, the 16-PLL enhanced formation of the long-chain branched structures of the PLL through the chain extension reaction. The star-shaped structure of 16-PLL also improved the melt flow property of the blends. The stress at break for 1-PLL films was improved by both the 16-PLL and chain extension reaction. It is of important for the application of PLL with crystallizability-melt flow property balance, which can be tailored by varying the 16-PLL blend ratio and chain extension reaction.

ACKNOWLEDGEMENT

This research was financially supported by Mahasarakham University Grant Year 2017 (Grant no. 6005028). The Center of Excellence for Innovation in Chemistry (PERCH-CIC), Office of the Higher Education Commission, Ministry of Education, Thailand is also acknowledged.

REFERENCES

1. Garlotta D. *J. Polym. Environ.*, **2001**, *9*, 63-84.
2. Auras, R.; Harte, B.; Selke, S. *Macromol. Biosci.*, **2003**, *4*, 835-864.
3. Lim, L. T.; Auras, R.; Rubino, M. *Prog. Polym. Sci.*, **2008**, *33*, 820-852.
4. Anderson, K. S.; Schreck, K. M.; Hillmyer, M. A. *Polym. Rev.*, **2008**, *48*, 85-108.
5. Saeidlou, S.; Huneault, M. A.; Li, H.; Park, C. B. *Prog. Polym. Sci.*, **2012**, *37*, 1657-1677.
6. Jaszkiewicz, A.; Bledzki, A. K.; Meljon, *Polym. Degrad. Stab.*, **2014**, *101*, 65-70.
7. Sarasua, J. R.; Arraiza, A. L.; Balerdi, P.; Maiza, I. *Polym. Eng. Sci.*, **2005**, *45*, 745-753.
8. Randal, J.R.; Cink, K.; Smith, J.C., Branching polylactide by reacting OH or COOH polylactide with epoxide acrylate (co)polymer. U.S. Patent No. US 7, 566, 753 B2, **2009**.
9. Plichta, A.; Jaskulski, T.; Lisowska, P.; Macios, K.; Kundys, A. *Polymer.,* **2015**, *72*, 307–316.
10. Najafi, N.; Heuzey, M.C.; Carreau, P.J.; Wood-Adams, M. *Polym. Degrad. Stab.*, **2012**, *97*, 554-565.
11. Cailloux, J.; Santona, O.O.; Franco-Urquiza, E.; Bou, J.J.; Carrasco, F.; Gamez-Perez, J.; Maspoch, M.L. *Express Polym. Lett.*, **2013**, *7*, 304-318.
12. Khajeheian, M. B.; Rosling, A. Preparation and characterization of linear and star-shaped poly L-lactide blends. *J. Appl. Polym. Sci.*, **2016**, *133*, 42231.
13. Pasee, S.; Cheerarot, O.; Baimark, Y. *Orient. J. Chem.*, **2015**, *31*, 1551-1558.
14. Zhang, C.; Zhai, T.; Turng, L. S.; Dan, Y. *Ind. Eng. Chem. Res.*, **2015**, *54*, 9505-9511.
15. Corre, Y. M.; Maazouz, A.; Reignier J.; Duchet, *J. Polym. Eng. Sci.*, **2014**, *54*, 616-625.
16. Baimark, Y.; Cheerarot, O. *Orient. J. Chem.*, **2015**, *31*, 635-641.
17. Perego, G.; Cella, G. B.; Bastioli, C. *J. Appl. Polym. Sci.*, **1996**, *59*, 37–43.